Physics of the Earth and Planetary Interiors 180 (2010) 244–257

Contents lists available at ScienceDirect

Physics of the Earth and Planetary Interiors

journal homepage: www.elsevier.com/locate/pepi

Geodynamical modeling and multiscale seismic expression of thermo-chemical heterogeneity and phase transitions in the lowermost mantle

Arie P. van den Berg[a,*], Maarten V. De Hoop[b], David A. Yuen[c], Anton Duchkov[d], Robert D. van der Hilst[e], Michael H.G. Jacobs[f]

[a] Dept. of Theoretical Geophysics, Institute of Earth Sciences, Utrecht University, 3508 TA Utrecht, The Netherlands
[b] Department of Mathematics and Center of Applied and Computational Mathematics, Purdue University, West Lafayette, IN, USA
[c] Department of Geology and Geophysics and Minnesota Supercomputing Institute, University of Minnesota, Minneapolis, MN, USA
[d] Department of Mathematics and Center of Applied and Computational Mathematics, Purdue University, West Lafayette, IN, USA
[e] Department of Earth Planetary Sciences, M.I.T., Cambridge, MA, USA
[f] Institut für Metallurgie, TU Clausthal, Clausthal-Zellerfeld, Germany

ARTICLE INFO

Article history:
Received 23 June 2009
Received in revised form 12 February 2010
Accepted 16 February 2010

Guest Editors
Kei Hirose
Thorne Lay
David Yuen

Editor
G. Helffrich

Keywords:
Mantle convection
Post-perovskite
Seismic imaging
Heterogeneity

ABSTRACT

The D″ region at the base of the mantle is characterized by seismologically inferred 3D heterogeneity, including multiple interfaces, localized low velocity zones, and anisotropy. The occurrence of the post-perovskite (PPV) phase transition with a steep Clapeyron slope of 11.5–13 MPa/K, close to the core–mantle boundary, is a prime candidate for explaining observed seismic layering in the D″. To examine the effect of the PPV phase transition on seismic structure we have carried out finite-element simulations with high-resolution (up to 3 km) in a cylindrical geometry. The rheology of the mantle has both Newtonian diffusion and non-Newtonian components, with a much greater propensity to non-Newtonian for PPV. From the temperature output we computed the 2D variations in shear wavespeed using a seismic equation of state based on mineral physics data. We then use a wave-packet decomposition of the wavespeed variations, which accounts for the events-to-stations illumination to obtain the seismic expressions of the geodynamically modeled structures. The results reveal lens-shaped PPV structures, much like the patterns obtained from seismic imaging with ScS data. A similar analysis of thermo-chemical anomalies from a subducting slab with crustal material shows that structures with a spatial scale of MORB crustal thickness produce characteristic features reminiscent of the small scale detail in the seismic imaging results. These experiments illustrate the high sensitivity of the seismic expression near the CMB to the wavespeed coefficients of the oceanic crust under high pressure conditions.

1. Introduction

The discovery of the post-perovskite (PPV) phase near the CMB (Murakami et al., 2004; Oganov and Ono, 2004; Shim et al., 2004) has stirred a vigorous debate on the origin of seismologically observed complexity in the so-called D″ layer and on the effect of this transition on mantle dynamics. Closely related issues include the relative effects of temperature and chemistry on the depth to and (seismic) visibility of the phase transition and the distortion of the phase boundary by thermal convection. We address this through a combined geodynamical and seismological study. Previous geodynamical modeling of heterogeneity in the D″ layer considered relatively long wavelength solutions, with horizontal wavelengths greater than 60 km (Nakagawa and Tackley, 2006). In our thermo-chemical convection models, which include the major phase transitions, the smallest length scale considered is 5 km. Moreover, to account for a realistic setting, we include the (chemical heterogeneity) effect of the presence of subducted MORB (mid ocean ridge basalt) in the D″ region. We then explore the seismic expression and detectability of these thermo-chemical heterogeneities with a (multiscale) wave-packet analysis.

Recent high resolution seismic imaging of the D″ layer reveals large scale lens-shaped structures (> 2000 km wide and > 100 km height) which have been interpreted as post-perovskite domains (van der Hilst et al., 2007). Besides clear top and bottom boundaries representative of a double crossing configuration of the mineral phase distribution (Hernlund et al., 2005) these seismic images also reveal small scale structures, both in the PPV lenses and in the perovskite background mantle. Such small scale structure would be in agreement with the observation of precursors to PKIKP or PKP (seismic waves that pass through Earth's core) produced by scattering

* Corresponding author at: Earth Sciences Department, Theoretical Geophysics, Budapestlaan 4, 3584 CD Utrecht, The Netherlands. Tel.: +31 30 253 5072.
E-mail address: berg@geo.uu.nl (A.P. van den Berg).

0031-9201/$ – see front matter © 2010 Elsevier B.V. All rights reserved.
doi:10.1016/j.pepi.2010.02.008

from structure in the lowermost mantle (Cleary and Haddon, 1972; Hedlin et al., 1997). The global variation in seismic array detections of such scattering (Van den Berg et al., 1978; Hedlin and Shearer, 2000) could point to a non-uniform melange of mantle material and MORB (Ohta et al., 2008; Xu et al., 2008; Konishi et al., 2009) produced by the deep subduction of oceanic lithosphere through geological time.

We model the interaction of subducting lithospheric slabs with the D″ region (in presence of the PPV transition and oceanic crust) and focus on the self-consistent generation of post-perovskite lens-shaped structures and their interaction with small scale lineament perturbations that represent subducted oceanic basalt. Since the Clapeyron slope of the PPV transition is still debated, we investigate the effect of the PPV phase transition on the distribution of mineral phases and the variations in seismic wavespeed and reflectivity both for a slope of 6 MPa/K (Catalli et al., 2009) and a slope of 11.5 MPa/K (Hirose and Sinmyo, 2006). In the presence of thermal anomalies of a few hundred K, the largest Clapeyron slope considered (11.5 MPa/K) implies rugged topography. To capture this complexity as well as the (fine scale) distribution of MORB the nodal point resolution of the model for computational modeling is about 3 km (10 km) in the vertical (horizontal) direction, which is slightly less than the spatial resolution from ScS (and SKKS) scattering (Wang et al., 2006, 2008). The rheology of the PPV phase is not yet well known, but there are indications that there is a greater propensity for non-linear dislocation creep in PPV (Oganov et al., 2005), which may result in a weakening by about an order of magnitude (Hunt et al., 2009). Our models are, therefore, based on a composite rheology by including both Newtonian diffusion creep and Non-Newtonian dislocation creep.

From the mineralogy and phase chemistry predicted by the convection model we calculate the spatial variation of seismic wavespeed and reflectivity in order to understand better how D″ would appear in seismic images and how sensitive these images are to changes in model parameter (such as the value of the Clapeyron slope) and the presence or absence of ancient crust material (MORB). This involves the decomposition of the thermal- and thermo-chemical structures into multiscale filters, or wave packets (Andersson et al., 2008; de Hoop et al., 2009; Duchkov et al., 2010). The results shown here reveal long wavelength structure that share characteristics with preliminary results of inverse scattering of ScS and SKKS data (Shang et al., 2009) and may inspire (and help the interpretation of) future large scale imaging efforts.

2. Convection modeling and seismic analysis

2.1. Description of the cartesian numerical model with curved boundary

Our model calculations are conducted for a 2D cylindrical domain in order to capture the effects arising from the curvature of the CMB region. The layout of the domain and physical parameterization is illustrated in Fig. 1.

The governing equations of the numerical model express conservation of mass, momentum and energy in the extended Boussinesq formulation. Symbols are explained in Table 1. The equations, written in cartesian coordinates, are:

$$\partial_j u_j = 0 \tag{1}$$

$$-\partial_i \Delta P + \partial_j \tau_{ij} = Ra\left(\alpha T - \sum_p \frac{Rb_p}{Ra}\Gamma_p\right) g(r) e_{ir} \tag{2}$$

$$\tau_{ij} = \eta(T, P, \tau, \phi_p)\left(\partial_j u_i + \partial_i u_j\right) \tag{3}$$

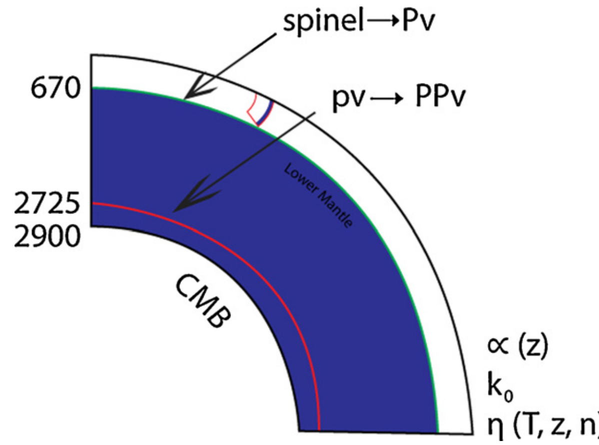

Fig. 1. Schematic diagram of the 90°cross-section of the cylindrical domain indicating the physical parameterizations used, including pressure (depth)-dependent thermal expansivity, uniform thermal conductivity and non-linear (with power-law index *n*) rheology, depending on stress, temperature, pressure and the mineral phase. The two major phase transitions included in the model are the spinel-post-spinel (perovskite + magnesiowuestite) at 670 km depth and the transition from perovskite to post-perovskite near the core–mantle boundary (CMB).

$$\frac{DT}{Dt} = \partial_j \partial_j T + \alpha Di w (T + T_0) + \sum_p \gamma_p \frac{Rb_p}{Ra} Di \frac{D\Gamma_p}{Dt}(T + T_0) + \frac{Di}{Ra}\Phi + RH(t) \tag{4}$$

The continuity equation (1) describes mass conservation of an incompressible fluid. The conservation of momentum is expressed in the Stokes equation (2) based on the infinite Prandtl number assumption, where $g(r)$ denotes the non-dimensional magnitude of the gravity acceleration and e_{ir}, $i = 1, 2$ are the direction cosines of the radial gravity acceleration vector. The constitutive equation (3) defines the non-linear temperature- and pressure-dependent viscous rheology which also depends on stress and mineral phase distribution as specified below. Energy transport is governed by (4), where the right-hand side terms are for thermal diffusion, adiabatic heating, latent heat of phase transitions, viscous dissipation and internal heating from radioactive elements, respectively.

Multiple phase transitions are implemented by using an extended Boussinesq formulation through the phase functions $\Gamma_p(P, T)$, which parameterize the Clapeyron curves in the phase diagram. This is expressed in the equation of state describing the phase transition (Christensen and Yuen, 1985),

$$\rho = \rho_0\left(1 - \alpha(T - T_{surf}) + \sum_p \Gamma_p \frac{\delta\rho_p}{\rho_0}\right) \tag{5}$$

As in Eqs. (2)–(4) index p in (5) runs over the three mineral phases included in the mantle model, representing (1) a phase for upper mantle olivine–spinel, (2) perovskite (PV) for most of the lower mantle and (3) post-perovskite (PPV) occurring in the bottom regions of the lower mantle. The parameterization of the phase boundaries is given in Tables 1 and 3.

For the numerical solution we apply finite-element methods to the coupled Stokes and energy equations. The incompressibility constraint (1) is taken into account through the use of a penalty function formulation for the Stokes equation, with penalty parameter $\epsilon = 10^{-9}$ (Cuvelier et al., 1986). For the Stokes equation we use quadratic (6-point) isoparametric elements, which allow an exact representation of the circular boundary of the computational domain (with a continuous normal vector). Fourfold subdivision